AMERICAN ACADEMY™
OF OPHTHALMOLOGY

Optical Coherence Tomography Angiography of Asymptomatic Neovascularization in Intermediate Age-Related Macular Degeneration

Luiz Roisman, MD,[1,2] Qinqin Zhang, PhD,[3] Ruikang K. Wang, PhD,[3] Giovanni Gregori, PhD,[1] Anqi Zhang, PhD,[3] Chieh-Li Chen, PhD,[3] Mary K. Durbin, PhD,[4] Lin An, PhD,[4] Paul F. Stetson, PhD,[4] Gillian Robbins, MS,[1] Andrew Miller, BS,[1] Fang Zheng, MD,[1] Philip J. Rosenfeld, MD, PhD[1]

Purpose: To determine whether angiography with swept-source (SS) optical coherence tomography (OCT) identifies subclinical type 1 neovascularization in asymptomatic eyes with intermediate age-related macular degeneration (iAMD).

Design: Prospective, observational, consecutive case series.

Participants: Patients with asymptomatic iAMD in one eye and neovascular age-related macular degeneration (AMD) in their fellow eye.

Methods: The patients underwent SS OCT angiography (OCTA), fluorescein angiography (FA), and indocyanine green angiography (ICGA), and the images from these 3 angiographic techniques were compared.

Main Outcome Measures: Identification of subclinical type 1 neovascularization with SS OCTA in asymptomatic eyes with iAMD.

Results: Eleven consecutive patients with iAMD in one eye and neovascular AMD in their fellow eye were imaged with FA, ICGA, and SS OCTA between August 2014 and September 2015. Clinical examination of the 11 eyes revealed drusen and pigmentary abnormalities in the central macula and no evidence of macular fluid on routine OCT imaging. Ten of the 11 eyes had no evidence of leakage on FA and 1 eye had questionable fluorescein leakage. Indocyanine green angiography revealed the presence of central macular plaques in 3 of the 11 asymptomatic eyes with iAMD, and SS OCTA revealed unambiguous type 1 neovascularization corresponding to the plaques in all 3 eyes. Optical coherence tomography angiography did not identify neovascularization in the remaining 8 eyes.

Conclusions: Swept-source OCTA identified type 1 neovascularization corresponding to ICGA plaques in asymptomatic eyes with iAMD. The ability of OCTA to provide noninvasive, fast, detailed, depth-resolved identification of nonexudative neovascular lesions in eyes with iAMD suggests the need for a new classification system that distinguishes between neovascular and nonneovascular iAMD. *Ophthalmology 2016;■:1–11 © 2016 by the American Academy of Ophthalmology.*

The onset of macular neovascularization (MNV) in age-related macular degeneration (AMD) defines the progression from intermediate, nonexudative AMD to late, exudative AMD, and this neovascularization has been divided into 3 types.[1] Type 1 and 2 neovascularization arise from the choroidal circulation and are referred to as choroidal neovascularization. Type 1 neovascularization exists beneath the Retinal pigment epithelium (RPE), and type 2 neovascularization is found between the retina and the RPE. Type 3 neovascularization arises from the retinal circulation and is also referred to as retinal angiomatous proliferation.[1]

Over the past decade, the management of MNV has been revolutionized by the introduction of drugs that inhibit vascular endothelial growth factor (VEGF).[2–5] Typically, anti-VEGF therapy is initiated after symptomatic exudation from MNV is confirmed by 1 or more imaging methods that include optical coherence tomography (OCT), fluorescein angiography (FA), and indocyanine green angiography (ICGA).

Historically, exudative AMD was diagnosed by the leakage of fluorescein from neovascularization.[6,7] Because fluorescein is a small molecule and only 20% of circulating fluorescein remains unbound to albumin, the leakage of fluorescein from both mature and immature vessels in the presence of excess VEGF serves as a useful marker for exudative neovascularization. Over the years, a detailed nomenclature has been developed to describe the different types of MNV based on their fluorescein leakage patterns, and their patterns have tended to correspond to the aggressiveness of the lesions.[7] In contrast to FA, ICGA uses a dye that is excited by near-infrared light, which has better penetration through the RPE. Because indocyanine green

© 2016 by the American Academy of Ophthalmology
Published by Elsevier Inc.

http://dx.doi.org/10.1016/j.ophtha.2016.01.044
ISSN 0161-6420/16

(ICG) is 98% protein bound, the dye does not usually leak from the neovascular lesions, and detailed imaging of type 1 neovascularization and the choroidal circulation is possible.[8] Thus, ICGA allows for visualization of the actual type 1 neovascular networks, and these lesions can be visualized as plaques during the late ICGA transit times. In 1998, Hanutsaha et al[9] reported the use of ICG videoangiography in 432 patients with neovascular AMD in one eye and nonexudative AMD in their fellow eye, and they found that 36 eyes (8%) had evidence of plaques in the nonexudative eye. In addition to using ICGA to detect plaques in asymptomatic eyes without exudation, histopathologic studies of autopsy eyes with presumed nonexudative AMD have identified subclinical fibrovascular tissue beneath the RPE in these eyes.[10,11] Currently, the exact incidence of plaques in asymptomatic eyes with presumed intermediate, nonexudative AMD using current ICGA techniques is not known, and it is unlikely such studies will be carried out given the systemic risks of ICGA, such as an allergic or anaphylactic reaction, the invasiveness and discomfort associated with ICGA, and the cost, all of which far outweigh the potential benefit of early detection because no therapy currently exists for these nonexudative lesions.

In contrast to FA and ICGA, OCT is easier to use; is noninvasive; is comparatively fast, safe, and less costly; and provides cross-sectional and en face images of macular anatomic features. As a result, OCT is the most widely used imaging technique for the screening, diagnosis, and management of late neovascular AMD.[6] Optical coherence tomography identifies MNV by the presence of structural changes within the macular layers that result from the leakage of fluid into the retina, under the retina, and under the RPE. Optical coherence tomography has proven useful for the detection and management of MNV because of its ability to follow the macular fluid noninvasively and its response to anti-VEGF therapy. However, with the development of OCT angiography (OCTA), it is now possible to image the actual neovascularization rather than just the VEGF-mediated fluid that leaks into the macula.

Optical coherence tomography angiography obtains multiple B-scans at the same position and detects erythrocyte movement based on changes in the intensity or phase information, or both, between B-scans.[12–15] This imaging strategy then is repeated at multiple, closely spaced positions within a defined area, and dense volumetric data sets are generated that can be used to create en face and cross-sectional images of the macular microvasculature without the need of exogenous dyes. A distinct advantage of OCTA compared with traditional angiography and routine intensity-based OCT imaging is the ability to detect MNV noninvasively before the macular anatomic features and the vision are disturbed. Early detection of MNV before leakage should result in better early monitoring of patients with intermediate AMD (iAMD) who are at high risk of conversion to late neovascular AMD. After all, early detection and treatment of pathologic neovascularization is thought to be important in preserving as much vision as possible in patients whose disease converts to exudative AMD. However, it is unclear at this time whether intervention before the lesion becomes symptomatic provides long-term visual acuity benefit.

In this study, we examined swept-source (SS) OCT microangiography (OMAG) images of patients diagnosed with neovascular AMD in one eye and asymptomatic, nonexudative AMD in their fellow eye. These patients had undergone ICGA for the neovascular disease in one eye, but images of their asymptomatic fellow eyes were obtained as well. In their asymptomatic eyes, ICGA revealed the presence of macular plaques, and these plaques were studied with SS OCTA.

Methods

Patients were enrolled at the Bascom Palmer Eye Institute in a prospective OCT imaging study. The institutional review board of the University of Miami Miller School of Medicine approved the study, and informed consent to participate in the prospective OCT study was obtained from all patients. The study was performed in accordance with the tenets of the Declaration of Helsinki and complied with the Health Insurance Portability and Accountability Act of 1996.

Optical coherence tomography angiography was performed using of a modified Cirrus prototype provided by Carl Zeiss Meditec, Inc. (Dublin, CA), containing an SS laser with a central wavelength of 1050 nm (1000−1100 nm full width) and a speed of 100 000 A-scans per second. The Zeiss 1050-nm SS OCT prototype had a full width at half maximum axial resolution of approximately 5 μm in tissue and a lateral resolution at the retinal surface estimated at approximately 14 μm. To image the retinal and choroidal vasculatures, a repeated B-mode scan protocol was used to acquire volumetric data sets, which then were processed using OMAG.[16–20] The OMAG algorithm used variations in both the intensity and phase information between sequential B-scans at the same position when creating an en face blood flow image. The OMAG scans were centered on the fovea and measured 3×3 mm on the retina. In the fast scanning direction (i.e., transverse, x-axis), 300 A-lines were used to form a single B-scan. Four consecutive B-scans were obtained at each fixed location before proceeding to the next transverse location on the retina. In the slow scanning direction (i.e., y-axis), there were 300 positions over a 3-mm distance. The spacing between adjacent B-scan positions was 10 μm. The time difference between 2 successive B-scans was roughly 3.8 ms, which corresponded to a B-scan acquisition rate of 263 B-scans per second.

The OMAG algorithm generates OCT angiograms that contain the retinal, choriocapillaris, and choroidal microvasculature, as well as the more usual OCT image containing the structural intensity information. A semiautomated macular slab segmentation algorithm was used on the structural OCT volume and the layer locations applied to the flow volumes to create an en face projection of the vascular networks in individual layers.[21] One layer was segmented between the bottom boundary of the outer plexiform layer and 8 μm beneath Bruch's membrane, therefore including the inner portion of the choriocapillaris. We called this slab the outer retinal layer. This segmentation scheme has been described previously.[20] Colors were used to code for different layers to give a better depth-encoded visualization of the neovascularization. The microvasculature from the outer retina to the choriocapillaris (CC) was colored pink and the rest of the choroidal vasculature was colored green. It is possible to see some projection artifacts of the retinal vasculature that were colored red. Structural B-scans also were generated in which each B-scan was averaged from the 4 repeated scans at the same position, shown as usual in

grayscale. These could be overlaid with color-coded OMAG B-scans to help visualization. On these images, the color red was used to represent both the superficial retinal vasculature, from the ganglion cell layer to the inner plexiform layer, and the choriocapillaris; green represented both the middle retinal vasculature, from the inner nuclear layer to the outer plexiform layer, and the choroidal vasculature, and pink represented the flow within the outer retinal layer. The 3-dimensional structure of the retina and its microvasculature were rendered and projected using Matlab software (The MathWorks, Natick, MA). The segmentation allowed for the visualization of the microvasculature in different layers of the retina and choroid, and a maximum projection method within each layer was used to create the en face images of interest. The projection artifacts were minimized for better visualization of the MNV using a technique described elsewhere.[22]

The qualitative OMAG en face images were compared with early- and late-phase FA and ICGA images. Abnormalities in the OMAG images were identified qualitatively based on deviations from the expected location, shape, size, and distribution of the microvasculature in the various layers. The averaged OCT B-scans also were examined in the usual manner, and the cross-sectional retinal images were compared with the en face intensity and flow images.

Consecutive patients with the diagnoses of neovascular AMD in one eye and nonexudative, iAMD in their fellow eye were enrolled and imaged between August 2014 and September 2015. In addition to OCT, patients with AMD also underwent a comprehensive ocular examination and imaging tests as part of their routine evaluation. The imaging tests included color fundus imaging (Topcon, Tokyo, Japan), autofluorescence, FA and ICG imaging (Heidelberg Engineering, Heidelberg, Germany), and spectral-domain (SD) OCT imaging (Cirrus; Carl Zeiss Meditec, Dublin, CA). Spectral-domain OCT imaging included the 200×200 macular raster scan pattern. Asymptomatic eyes with subclinical MNV were identified by the presence of an ICGA plaque in the absence of visual symptoms. This finding was confirmed by at least 2 retina specialists (L.R. and P.J.R.). Plaques were identified by ICGA imaging as well-delineated areas of increased fluorescence measuring at least 0.5 disc area in size within the central macula and most evident during the late transit frames of the ICGA imaging study.

Results

Eleven patients with neovascular AMD in one eye and asymptomatic iAMD in the fellow eye underwent FA and ICGA, in addition to research imaging using the Zeiss prototype 1-μm SS OCT instrument. Indocyanine green angiography revealed the presence of central macular plaques in 3 of the fellow asymptomatic eyes. Their clinical evaluation showed drusen and pigmentary abnormalities in the central macula and no evidence of macular fluid on OCT. One patient had questionable leakage on FA from the asymptomatic eye. Swept-source OMAG revealed type 1 neovascularization corresponding to the plaques in all 3 cases. For each case, the accompanying figures show the early and late frames of the FA and ICGA along with the en face subretinal flow images from the outer retina to the choriocapillaris layers. Two representative B-scans are shown, one depicting the typical intensity image and the other showing the same B-scan with layer-specific, color-coded microvascular flow information superimposed on the intensity image.

Patient 1

A 78-year-old man reported blurred vision in his left eye. Best-corrected visual acuity was 20/20 and 20/25 in the right and left eyes, respectively. Upon evaluation, the left eye was diagnosed with new-onset MNV. The right eye was asymptomatic, and on routine SD OCT B-scan imaging, there was no evidence of macular fluid. Color fundus and autofluorescence imaging, FA, and ICGA were performed (Fig 1A–F). Color fundus imaging revealed central drusen and pigmentary changes along with perimacular reticular pseudodrusen (RPD), which also were evident on autofluorescence imaging (Fig 1A, B). Fluorescein angiography showed some punctate areas of hyperfluorescence without leakage (Fig 1C, D). Indocyanine green angiography imaging also confirmed the presence of RPD and revealed a subfoveal plaque (Fig 1E, F). Swept-source OCTA imaging was performed (Fig 2A–F). The typical cross-sectional intensity-based B-scan images revealed small RPE elevations consistent with typical drusen (Fig 2A). However, the cross-sectional and en face SS OCTA images showed evidence of flow within the presumed drusen (Fig 2B), and the en face images revealed a multilobular neovascular lesion occupying the same position as the plaque (Fig 2D–F). The en face flow image corresponded well with the magnified image of the ICGA plaque from the same area of the macula imaged using SS OMAG (Fig 2C).

Patient 2

An 82-year-old woman reported worsening vision in the left eye. She had a history of anti-VEGF injections in her left eye for neovascular AMD, with the last injection given 5 months previously. Best-corrected visual acuity was 20/20 and 20/300 in the right and left eyes, respectively. Color fundus and autofluorescence imaging, FA, ICGA, and OCT were performed, and recurrent neovascular activity was diagnosed in the left eye. On color fundus and autofluorescence imaging, the asymptomatic right eye showed evidence of macular drusen and pigmentary abnormalities along with RPD (Fig 3A, B). Early and late transit frames from FA revealed evidence of focal hyperfluorescence early with late staining consistent with nonexudative AMD (Fig 3C, D). Early and late transit frames from the ICGA revealed a central macular plaque with foveal sparing (Fig 3E, F). Both the FA and ICGA images show RPD surrounding the central macula. Swept-source OCTA was performed (Fig 4A–F). The typical cross-sectional intensity-based B-scan images revealed low-lying RPE elevations consistent with typical drusen (Fig 4A). However, the cross-sectional and en face SS OCT angiographic images revealed evidence of flow within the presumed drusen (Fig 4B), and the en face images revealed a circular neovascular lesion with foveal sparing occupying the same position as the plaque (Fig 4D–F). The en face flow image corresponded well with the magnified image of the ICGA plaque from the same area of the macula imaged using SS OMAG (Fig 4C).

Patient 3

An 81-year-old man reported blurred vision in his right eye. Best-corrected visual acuity was 20/100 and 20/30 in the right and left eyes, respectively. Color fundus and autofluorescence imaging, FA, and ICGA were performed. The right eye was diagnosed with MNV. Figure 5 shows the images of the asymptomatic left eye. Color fundus and autofluorescence imaging revealed some typical drusen and pigmentary changes, and the left eye was diagnosed with iAMD (Fig 5A, B). Early and late transit frames from the FA revealed evidence of stippled hyperfluorescence with questionable late leakage (Fig 5C, D). Early and late transit frames from the ICGA revealed a central macular plaque (Fig 5E, F).

Swept-source OCTA was performed (Fig 6A–F). The typical cross-sectional intensity-based B-scan images revealed RPE elevations consistent with typical drusen (Fig 6A). However, the

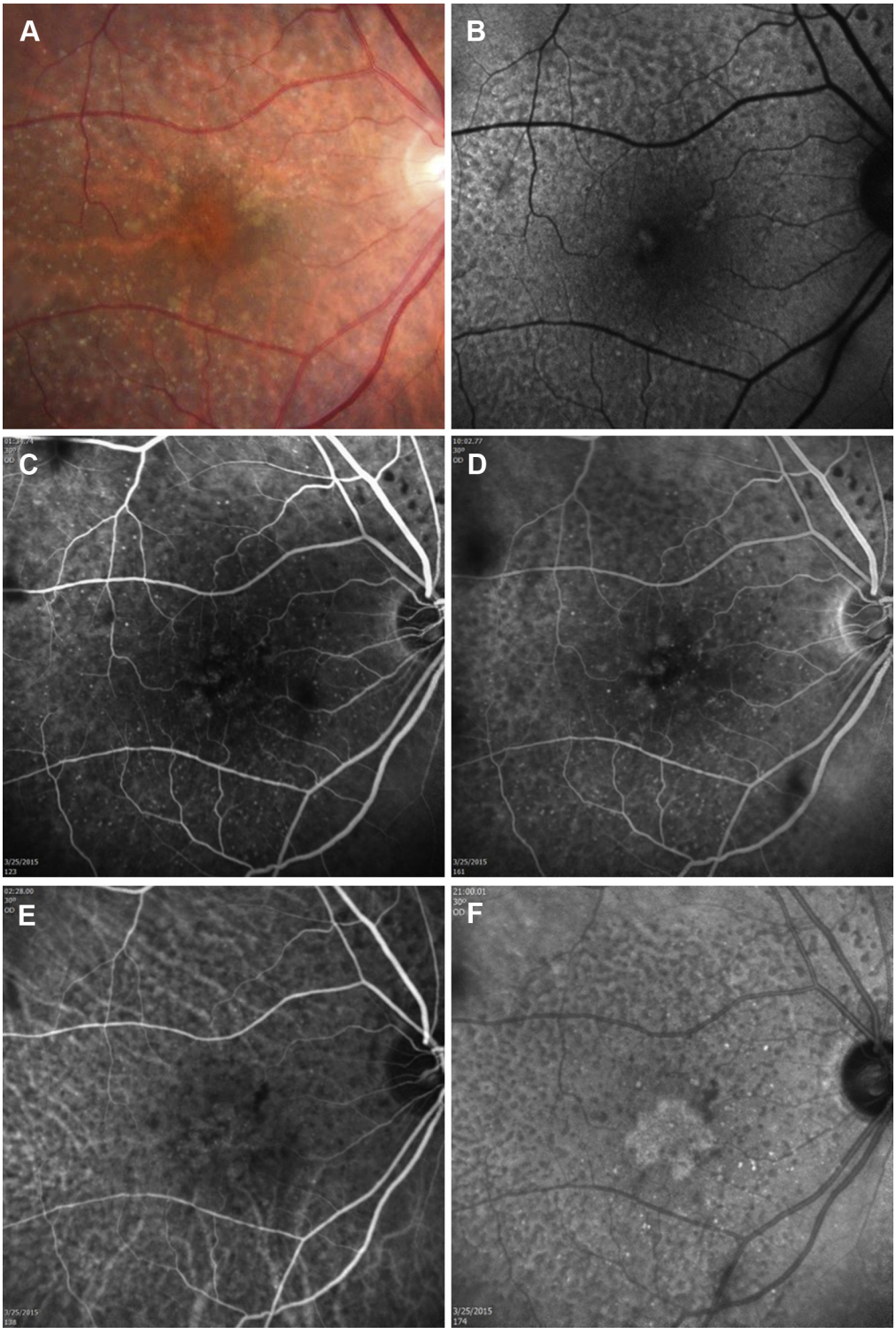

Figure 1. Images showing an asymptomatic eye from patient 1, who had exudative age-related macular degeneration in the fellow eye. **A**, Color fundus imaging showing drusen, pigmentary abnormalities, and reticular pseudodrusen (RPD). **B**, Autofluorescence imaging showing RPD. **C**, **D**, Early and late frames from a fluorescein angiogram showing some early focal hyperfluorescence, but no obvious late leakage, and RPD surrounding the central macula. **E**, **F**, Early and late frames from an indocyanine green angiogram showing a central plaque in the late frames and RPD surrounding the central macula.

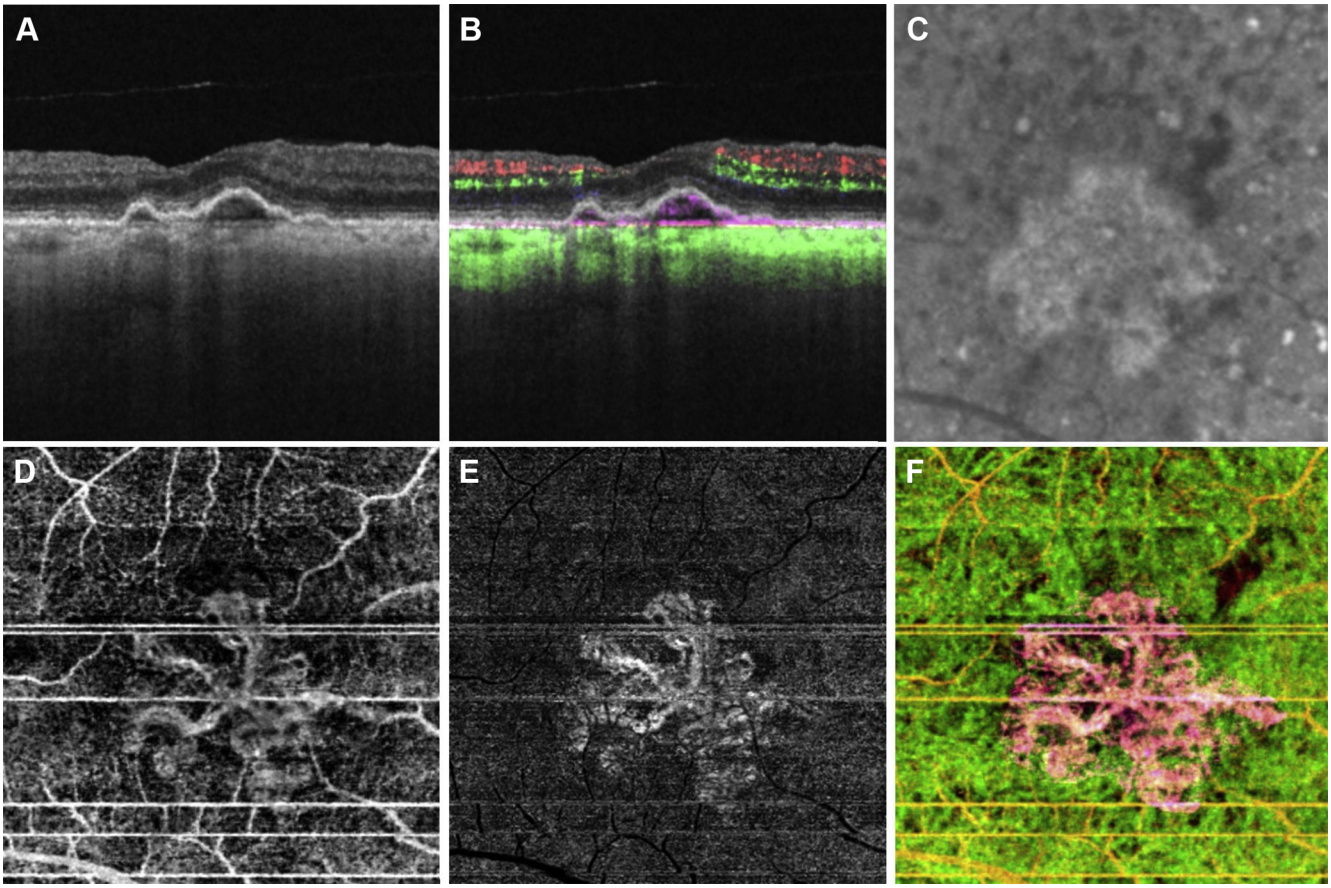

Figure 2. Swept-source (SS) optical coherence tomography microangiography (OMAG) of an asymptomatic eye from patient 1, who had exudative age-related macular degeneration in the fellow eye. **A**, Standard optical coherence tomography (OCT) B-scan through the fovea showing elevations of the retinal pigment epithelium (RPE) consistent with typical drusen, but no evidence of macular fluid. **B**, Standard OCT B-scan through the fovea with color-coded flow represented as red and green for the retinal microvasculature, pink for flow under the RPE and within the inner choriocapillaris and green for flow in the remainder of the choroid. Note the pink coloration under the RPE elevations that were thought to be a typical drusen on the routine OCT B-scan. **C**, Magnified area of the plaque seen on a late indocyanine green angiography image corresponding to the same area scanned by SS OMAG. **D**–**F**, Swept-source OMAG en face images of a slab within the outer retinal layer (ORL) that was between the bottom boundary of the outer plexiform layer and 8 μm beneath the Bruch's membrane. **D**, Swept-source OMAG en face image showing a multilobular neovascular complex observed using the ORL slab. **E**, The same en face image shown in (**D**) after removal of projection artifacts. **F**, Composite, color-coded en face SS OMAG flow image encompassing the ORL and the choroid, revealing the multilobular type 1 neovascularization in pink.

cross-sectional and en face SS OCTA images revealed evidence of flow within the presumed drusen (Fig 6B), and the en face images revealed a multilobular neovascular lesion occupying the same position as the plaque (Fig 6D–F). The en face flow image corresponded well with the magnified image of the ICGA plaque from the same area of the macula imaged using SS OMAG (Fig 6C).

Discussion

The presence of ICG plaques in the absence of obvious clinical, angiographic, or OCT signs of exudation in eyes with AMD has been described previously.[9,23] These subclinical ICG plaques have been reported to enlarge over time without significant changes in macular thickness, macular sensitivity, retinal anatomic features, or visual acuity.[23,24] However, the detection of subclinical MNV required the use of ICGA, which is an invasive procedure associated with the rare but serious risk of an allergic or anaphylactic reaction. Moreover, ICGA is expensive, time consuming, resource intensive, uncomfortable for the patient, and not routinely performed or reimbursed by insurance plans when performed on patients with nonexudative AMD. Because of these limitations, angiographic monitoring of eyes with iAMD has never become routine; however, this is about to change with the availability of OCTA.

In the 3 case reports presented in this study, asymptomatic eyes with iAMD were imaged with ICGA because the patient was being evaluated for active, symptomatic neovascularization in their fellow eye. When images from the Zeiss 1050-nm SS OCT prototype system were processed using the OMAG algorithm, type 1 neovascularization was identified and its location corresponded to the central macular plaque seen on ICGA imaging. In our patients, the presence of MNV would have remained unnoted if the ICGA had not been performed and subsequently confirmed by OCTA. Although

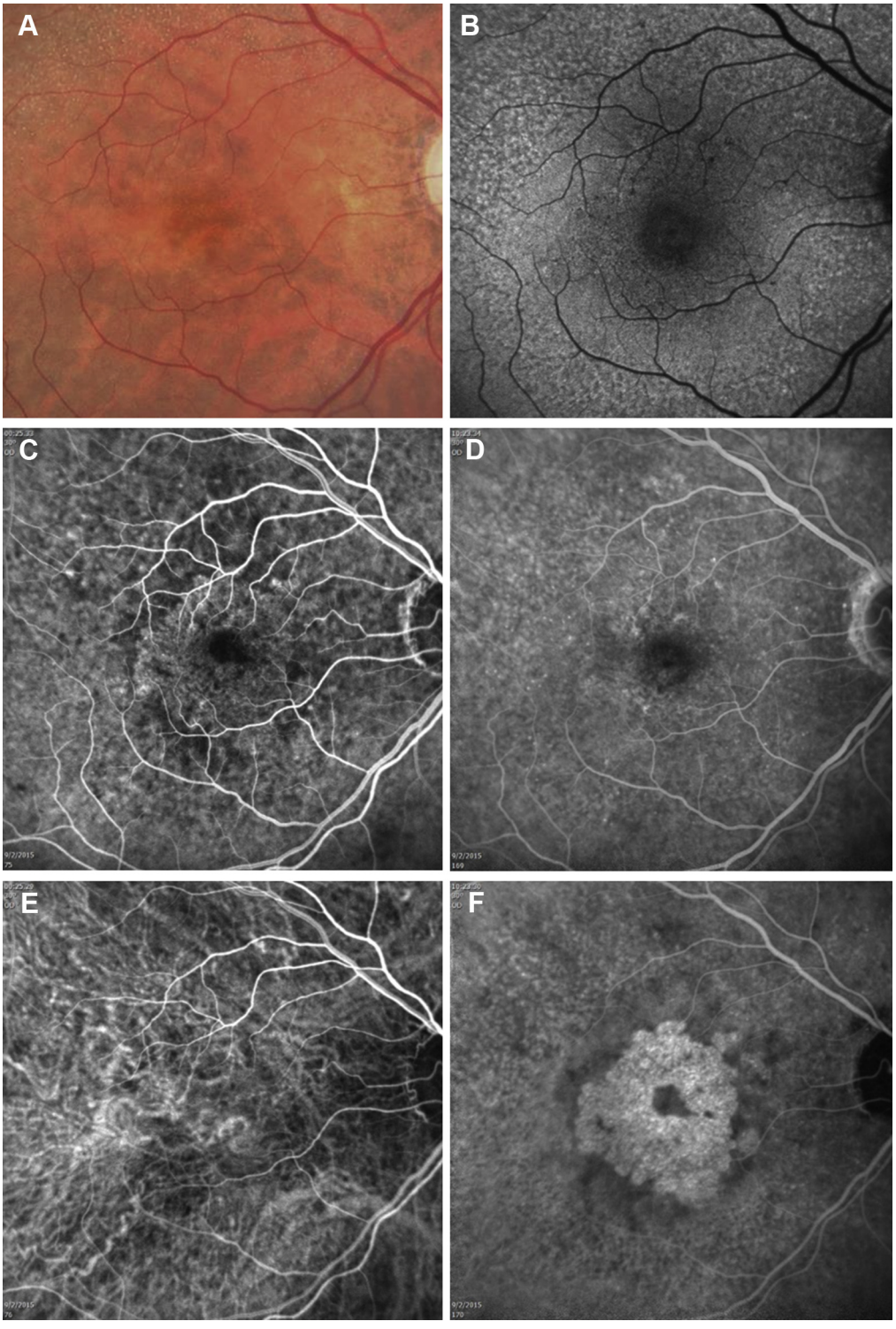

Figure 3. Images showing an asymptomatic eye from patient 2, who had exudative age-related macular degeneration in the fellow eye. **A**, Color fundus imaging showing drusen, pigmentary abnormalities, and reticular pseudodrusen (RPD). **B**, Autofluorescence imaging showing RPD. **C**, **D**, Early and late frames from a fluorescein angiogram showing some early focal hyperfluorescence, but no obvious late leakage, and RPD surrounding the central macula. **E**, **F**, Early and late frames from an indocyanine green angiogram showing a central plaque in the late frames and RPD surrounding the central macula.

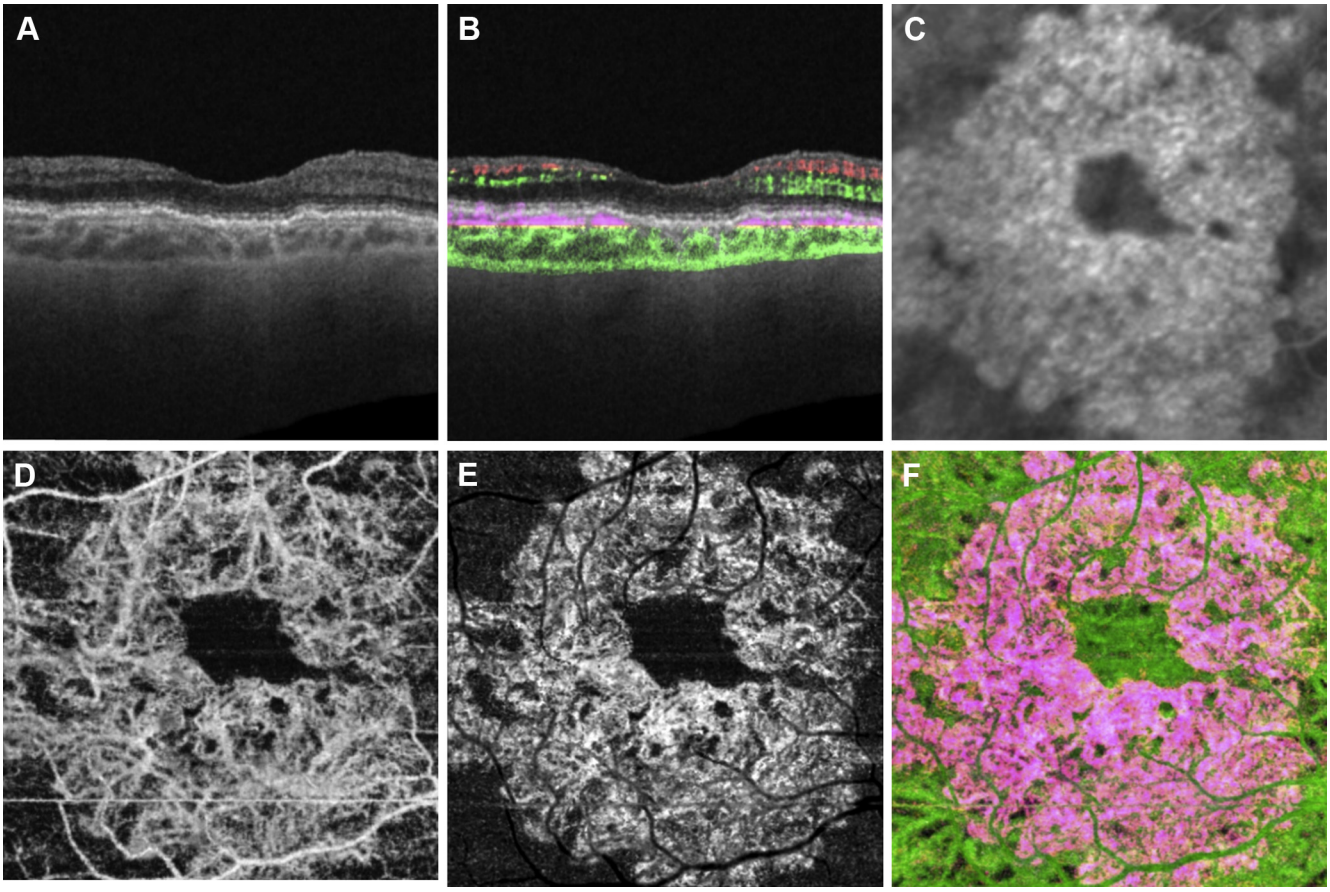

Figure 4. Swept-source (SS) optical coherence tomography microangiography (OMAG) of an asymptomatic eye from patient 2, who had exudative age-related macular degeneration in the fellow eye. **A**, Standard optical coherence tomography (OCT) B-scan through the fovea showing elevations of the retinal pigment epithelium (RPE) consistent with typical drusen, but no evidence of macular fluid. **B**, Standard OCT B-scan through the fovea with color-coded flow represented as red and green for the retinal microvasculature, pink for flow under the RPE and within the inner choriocapillaris, and green for flow in the remainder of the choroid. Note the pink coloration under the RPE elevations that were thought to be a typical, confluent drusen on the routine OCT B-scan. **C**, Magnified area of the plaque seen on a late indocyanine green angiography image corresponding to the same area scanned by SS OMAG. **D**–**F**, Swept-source OMAG en face images of the outer retinal layer (ORL) slab, which was between the bottom boundary of the outer plexiform layer and 8 μm beneath the Bruch's membrane. **D**, Swept-source OMAG en face image showing a circular neovasculature complex observed using the ORL slab. **E**, The same en face image showed in (**D**) after removal of projection artifacts. **F**, Composite, color-coded en face SS OMAG flow image encompassing the ORL and the choroid revealing the circular type 1 neovascularization in pink.

other authors have found nonexudative MNV using OCTA under RPE detachments in eyes with nonexudative AMD,[25,26] in this report we diagnosed based on the presence of ICGA plaques and then the MNV was confirmed by SS OCTA. Evidence to support the conclusion that the SS OCTA flow patterns actually represent MNV includes the presence of ICGA plaques serving as positive controls for the presence of MNV; the correlations between the flow patterns and the presence, configurations, dimensions, and locations of the ICG plaques; and the correlations between the flow patterns and the dimensions of the pigment epithelial detachments (PED). Moreover, the flow patterns did not correlate with any known normal vascular flow pattern in this region, and a similar flow pattern was not observed in the absence of a plaque. Consequently, these correlations between the SS OCTA flow images, the ICGA images, and the OCT anatomic images strongly support the conclusion that these SS OCTA images represented MNV.

Overall, we found that 3 of the 11 eyes (27%) harbored previously undetected MNV. This may explain why the incidence rate of exudative lesions in these eyes with iAMD has been reported to be higher than the incidence rates of MNV in patients with iAMD in both eyes.[27] Moreover, this subclinical MNV seems to be contained within irregular elevations of the RPE that had been diagnosed as typical drusen on routine OCT imaging.[23] However, the irregular, low-lying elevations of the RPE actually represented fibrovascular RPE detachments containing reflective material that corresponded to the neovascularization. This OCT configuration is likely to be indicative of subclinical MNV, rather than just coalescent drusen. Thus, although it is not possible to identify with certainty whether a small, low-lying irregular PED is vascularized using routine OCT imaging, the use of SS OMAG should be able to distinguish between vascularized and nonvascularized lesions and replace ICGA for the identification of plaques in the central

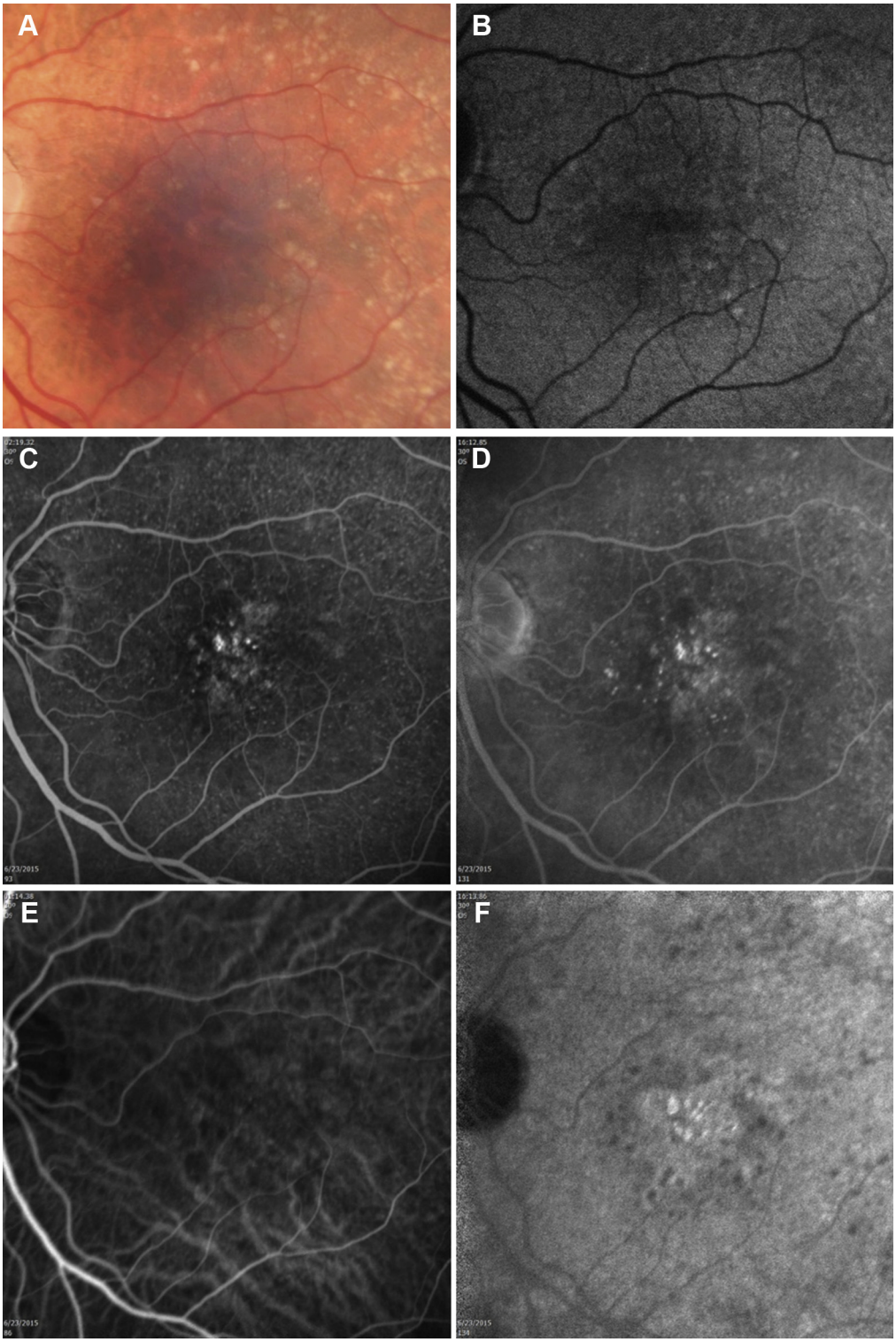

Figure 5. Images of an asymptomatic eye from patient 3, who had exudative age-related macular degeneration in the fellow eye. **A**, Color fundus imaging showing drusen and pigmentary abnormalities. **B**, Autofluorescence imaging showing reticular pseudodrusen more evident around the superior arcade. **C**, **D**, Early and late frames from a fluorescein angiogram showing some early stippled hyperfluorescence and subtle late leakage consistent with type 1 neovascularization. **E**, **F**, Early and late frames from an indocyanine green angiogram showing a central multilobular plaque in the late frames.

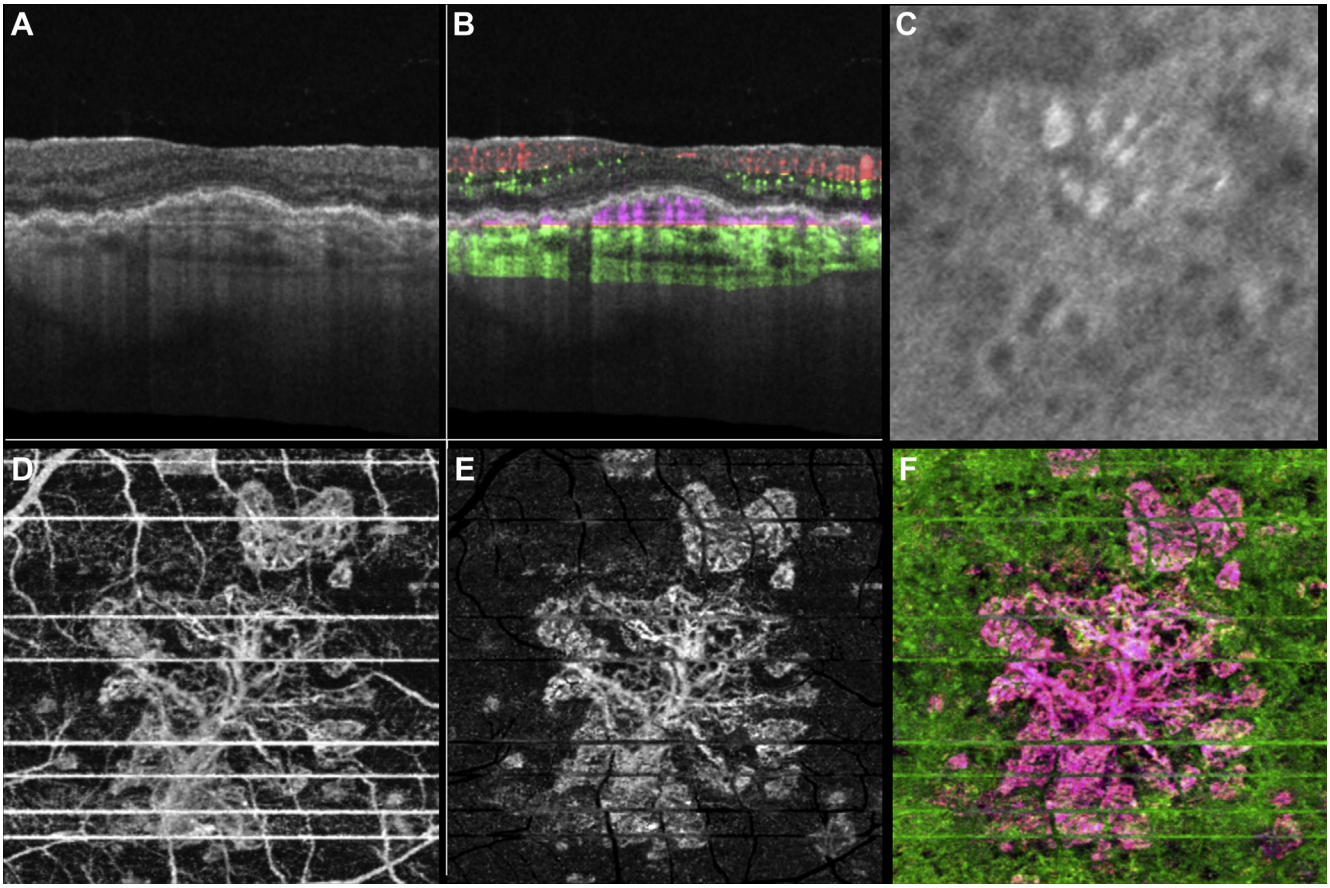

Figure 6. Swept-source (SS) optical coherence tomography microangiography (OMAG) of an asymptomatic eye from patient 3, who had exudative age-related macular degeneration in the fellow eye. **A**, Standard optical coherence tomography (OCT) B-scan through the fovea showing elevations of the retinal pigment epithelium (RPE) consistent with typical, confluent drusen, but no evidence of macular fluid. **B**, Standard OCT B-scan through the fovea with color-coded flow represented as red and green for the retinal microvasculature, pink for flow under the RPE and within the inner choriocapillaris, and green for flow in the remainder of the choroid. Note the pink coloration under the RPE elevations that were thought to be a typical drusen on the routine OCT B-scan. **C**, Magnified area of the plaque seen on a late indocyanine green angiography image corresponding to the same area scanned by SS OMAG. **D–F**, Swept-source OMAG en face images of the outer retinal layer (ORL) slab, which was between the bottom boundary of the outer plexiform layer and 8 μm beneath the Bruch's membrane. **D**, Swept-source OMAG en face image showing a multilobular neovasculature complex observed using the ORL slab. **E**, The same en face image shown in (**D**) after removal of projection artifacts. **F**, Composite, color-coded en face SS OMAG flow image encompassing the ORL and the choroid revealing the circular type 1 neovascularization in pink.

macula. Moreover, a new terminology is needed to describe the different stages of AMD. One possibility would be to subdivide iAMD into nonneovascular iAMD and neovascular iAMD, with the actual development of exudation signaling the progression to late AMD.

The use of SS OMAG to diagnose subclinical type 1 neovascularization has some obvious advantages when following up patients with all forms of AMD and for screening patients to be enrolled in clinical trials, particularly patients being included in trials designed to test new treatments for nonexudative AMD. The significant advantage of SS OMAG over ICGA is that it can be repeated easily at follow-up visits because it is fast, safe, and noninvasive. With the widespread availability of OCTA, it will be possible to answer many of the questions surrounding these subclinical neovascular lesions, such as their prevalence, their natural history before they become symptomatic, and their response to anti-VEGF therapy while the fellow eye is being treated. There is a growing concern that these asymptomatic neovascular lesions will be treated aggressively with anti-VEGF therapy before the natural history data are acquired. To address these concerns, we recommend that anti-VEGF therapy not be performed on these asymptomatic eyes in routine clinical care and only be performed within the context of a clinical trial. Although it seems reasonable to assume that these eyes are more likely to progress to active, symptomatic forms of exudative AMD, questions remain about their natural history and the consequences of anti-VEGF therapy at this stage. One possibility is that these asymptomatic lesions may be providing nutritional support for the overlying RPE and photoreceptors, and anti-VEGF therapy could promote the formation of macular atrophy. Other considerations if therapy is initiated include the appropriate goal of therapy, how often the treatment should be given, and what the rules would be for curtailing therapy if no exudation or vision loss is observed. Until data from

natural history studies are available, these eyes should be followed up more closely than eyes without evidence of subclinical MNV because of the presumed increased risk of exudation and vision loss. Additionally, when recruiting nonexudative AMD patients into clinical trials, it would be worthwhile to stratify patients at baseline with OCTA available to determine whether subclinical MNV is present to understand better the effect of new treatments on these lesions. After all, if these eyes with subclinical MNV are not balanced between treatment groups at baseline, then the results of these trials may be confounded, especially if subclinical neovascularization responds differently to emerging therapies, such as the next-generation subthreshold laser treatments or drugs for nonexudative AMD. Moving forward, it seems reasonable to include OCT angiography as an imaging technique to be performed at baseline and at follow-up visits in all trials enrolling patients with nonexudative AMD.

The limitations of this study include the small number of eyes and the lack of a fully automated algorithm. The small sample size reflects the decreasing use of ICGA in neovascular AMD patients, but now that we have correlated ICGA plaques with SS OCTA flow images, we plan to move forward and determine the incidence of subclinical MNV based on SS OCTA imaging alone. Whether ICGA or SS OCTA is more sensitive in detecting these lesions remains to be determined and should be addressed in a large natural history study. A current limitation of the high-density SS OCT imaging strategy used in this research is that the scan area measures only 3×3 mm within the central macula. Another limitation of this research is that we did not determine whether OCTA performed with commercially available SD OCT instruments could detect these cases of asymptomatic MNV as well as our SS OCT instrument. Because SS OCT and SD OCT instruments differ with respect to their light sources, central wavelengths, scanning speeds, scan densities, scanning areas, motion correction strategies, and segmentation algorithms, this type of comparison needs to be carried out; however, it was outside the scope of this research because the commercially available SD OCTA instrument was not yet available to us when the patients in this report were enrolled and imaged. As this technology evolves and faster scanning rates are achieved, the ability to scan larger areas and areas outside the central macula should become available routinely.

In summary, our results demonstrate the usefulness of SS OCTA for the diagnosis of subclinical type 1 neovascularization in asymptomatic eyes with presumed iAMD. The ability to detect subclinical neovascularization easily in these eyes suggests that iAMD needs to be classified as either nonneovascular or neovascular iAMD. With the growing availability of OCTA, it seems likely that traditional FA and ICGA will no longer be needed for AMD patients with central macular lesions. The ability to acquire both structure and flow information noninvasively from a single OCT data set suggests that OCT imaging will replace most, if not all, of the current imaging now performed using dye-based angiography for the routine management of AMD patients.

References

1. Freund KB, Zweifel SA, Engelbert M. Do we need a new classification for choroidal neovascularization in age-related macular degeneration? Retina 2010;30:1333–49.
2. Brown DM, Kaiser PK, Michels M, et al. Ranibizumab versus verteporfin for neovascular age-related macular degeneration. N Engl J Med 2006;355:1432–44.
3. Rosenfeld PJ, Brown DM, Heier JS, et al. Ranibizumab for neovascular age-related macular degeneration. N Engl J Med 2006;355:1419–31.
4. Comparison of Age-Related Macular Degeneration Treatments Trials Research Group, Martin DF, Maguire MG, Fine SL, et al. Ranibizumab and bevacizumab for treatment of neovascular age-related macular degeneration: two-year results. Ophthalmology 2012;119:1388–98.
5. Yannuzzi LA, Freund KB, Takahashi BS. Review of retinal angiomatous proliferation or type 3 neovascularization. Retina 2008;28:375–84.
6. Gess AJ, Fung AE, Rodriguez JG. Imaging in neovascular age-related macular degeneration. Semin Ophthalmol 2011;26:225–33.
7. Barbazetto I, Burdan A, Bressler NM, et al. Photodynamic therapy of subfoveal choroidal neovascularization with verteporfin: fluorescein angiographic guidelines for evaluation and treatment—TAP and VIP report no. 2. Arch Ophthalmol 2003;121:1253–68.
8. Flower RW. Extraction of choriocapillaris hemodynamic data from ICG fluorescence angiograms. Invest Ophthalmol Vis Sci 1993;34:2720–9.
9. Hanutsaha P, Guyer DR, Yannuzzi LA, et al. Indocyanine-green videoangiography of drusen as a possible predictive indicator of exudative maculopathy. Ophthalmology 1998;105:1632–6.
10. Green WR, McDonnell PJ, Yeo JH. Pathologic features of senile macular degeneration. Ophthalmology 1985;92:615–27.
11. Spraul CW, Grossniklaus HE. Characteristics of drusen and Bruch's membrane in postmortem eyes with age-related macular degeneration. Arch Ophthalmol 1997;115:267–73.
12. Makita S, Hong Y, Yamanari M, et al. Optical coherence angiography. Opt Express 2006;14:7821–40.
13. Jia Y, Tan O, Tokayer J, et al. Split-spectrum amplitude-decorrelation angiography with optical coherence tomography. Opt Express 2012;20:4710–25.
14. Moult E, Choi W, Waheed NK, et al. Ultrahigh-speed swept-source OCT angiography in exudative AMD. Ophthal Surg Lasers Imag Retina 2014;45:496–505.
15. Nagiel A, Sadda SR, Sarraf D. A promising future for optical coherence tomography angiography. JAMA Ophthalmol 2015;133:629–30.
16. Huang Y, Zhang Q, Thorell MR, et al. Swept-source OCT angiography of the retinal vasculature using intensity differentiation-based optical microangiography algorithms. Ophthal Surg Lasers Imag Retina 2014;45:382–9.
17. An L, Subhush HM, Wilson DJ, Wang RK. High-resolution wide-field imaging of retinal and choroidal blood perfusion with optical microangiography. J Biomed Opt 2010;15:026011.
18. Wang RK, An L, Francis P, Wilson DJ. Depth-resolved imaging of capillary networks in retina and choroid using ultrahigh sensitive optical microangiography. Opt Lett 2010;35:1467–9.
19. Wang RK, Jacques SL, Ma Z, et al. Three dimensional optical angiography. Opt Express 2007;15:4083–97.

20. Zhang Q, Wang RK, Chen CL, et al. Swept source Optical Coherence Tomography angiography of neovascular macular telangiectasia type 2. Retina 2015;35:2285–99.
21. Yin X, Chao JR, Wang RK. User-guided segmentation for volumetric retinal optical coherence tomography images. J Biomed Opt 2014;19:086020.
22. Zhang Anqi, Zhang Q, Wang RK. Minimizing projection artifacts for accurate presentation of choroidal neovascularization in OCT micro-angiography. Biomed Opt Express 2015;6:4130–43.
23. Querques G, Srour M, Massamba N, et al. Functional and multimodal imaging of treatment-naive "quiescent" choroidal neovascularization. Invest Ophthalmol Vis Sci 2013;54:6886–92.
24. Querques G, Tran TH, Forte R, et al. Anatomic response of occult choroidal neovascularization to intravitreal ranibizumab: a study by indocyanine green angiography. Graefes Arch Clin Exp Ophthalmol 2012;250:479–84.
25. Dansingani KK, Balaratnasingam C, Klufas MA, et al. Optical coherence tomography angiography of shallow irregular pigment epithelial detachments in pachychoroid spectrum disease. Am J Ophthalmol 2016 Jan 4. pii: S0002-9394(15)30024-6. doi: 10.1016/j.ajo.2015.12.019. [Epub ahead of print].
26. Palejwala NV, Jia Y, Gao SS, et al. Detection of nonexudative choroidal neovascularization in age-related macular degeneration with optical coherence tomography angiography. Retina 2015;35:2204–11.
27. Friberg TR, Bilonick RA, Brennen PM. Risk factors for conversion to neovascular age-related macular degeneration based on longitudinal morphologic and visual acuity data. Ophthalmology 2012;119:1432–7.

Footnotes and Financial Disclosures

Originally received: October 27, 2015.
Final revision: January 23, 2016.
Accepted: January 27, 2016.
Available online: ■■■. Manuscript no. 2015-1883.

[1] Department of Ophthalmology, Bascom Palmer Eye Institute, University of Miami Miller School of Medicine, Miami, Florida.

[2] Department of Ophthalmology, Federal University of São Paulo, São Paulo, Brazil.

[3] Department of Bioengineering, University of Washington, Seattle, Washington.

[4] Advanced Development, Carl Zeiss Meditec, Inc., Dublin, California.

Financial Disclosure(s):
The author(s) have made the following disclosure(s): R.K.W.: Financial support - Carl Zeiss Meditec, Inc (Dublin, CA); Patent (with Oregon Health & Science University, Portland, OR) - Carl Zeiss Meditec, Inc.

G.G.: Financial support - Carl Zeiss Meditec, Inc, (Dublin, CA); Patent (with University of Miami, Miami, FL) - Carl Zeiss Meditec, Inc.

M.K.D.: Employee - Carl Zeiss Meditec, Inc (Dublin, CA)

L.A.: Employee - Carl Zeiss Meditec, Inc (Dublin, CA)

P.F.S.: Employee - Carl Zeiss Meditec, Inc (Dublin, CA)

P.J.R.: Consultant - Achillion; Acucela; Alcon; Bayer; Chengdu Kanghong Biotech; CoDa Therapeutics; Genentech/Roche; Healios K.K.; Merck; Regeneron; Stealth; Tyrogenex; Supported by Acucela; Apellis; Genentech/Roche; GlaxoSmithKline; Neurotech; Ocata Therapeutics; Tyrogenex.

Supported by Carl Zeiss Meditec, Inc. (Dublin, CA); the National Eye Institute, National Institutes of Health, Bethesda, MD (grant no.: R01EY024158; and center core grant no.: P30EY014801 [Department of Ophthalmology, University of Miami Miller School of Medicine]); the Macula Vision Research Foundation (West Conshohocken, PA); the Emma Clyde Hodge Memorial Foundation; the Feig Family Foundation; Research to Prevent Blindness, Inc., New York, New York (unrestricted grant and innovative research award to R.K.W.); and the CAPES Foundation, Ministry of Education of Brazil, Brasília, DF, Brazil (L.R.).

Author Contributions:

Conception and design: Roisman, Gregori, Rosenfeld

Analysis and interpretation: Roisman, Q.Zhang, Wang, Gregori, A.Zhang, Chen, Durbin, An, Stetson, Robbins, Miller, Zheng, Rosenfeld

Data collection: Roisman, Q.Zhang, Wang, A.Zhang, Chen, An, Robbins, Miller, Zheng

Obtained funding: none

Overall responsibility: Roisman, Gregori, Rosenfeld

Abbreviations and Acronyms:
AMD = age-related macular degeneration; **FA** = fluorescein angiography; **iAMD** = intermediate age-related macular degeneration; **ICG** = indocyanine green; **ICGA** = indocyanine green angiography; **MNV** = macular neovascularization; **OCT** = optical coherence tomography; **OCTA** = optical coherence tomography angiography; **OMAG** = optical coherence tomography microangiography; **ORL** = outer retinal layer; **RPD** = reticular pseudodrusen; **RPE** = retinal pigment epithelium; **SD** = spectral-domain; **SS** = swept-source; **VEGF** = vascular endothelial growth factor.

Correspondence:
Philip J. Rosenfeld, MD, PhD, Department of Ophthalmology, Bascom Palmer Eye Institute, University of Miami Miller School of Medicine, 900 NW 17th Street, Miami, FL 33136. E-mail: prosenfeld@miami.edu.